Chapter 5

One-dimensional Faceting

As an essential result of the previous chapter it has been shown that ideal layer growth occurs for ionic insulator films on stepped metal surfaces if the spacing of the ionic charges in the film matches with the intrinsic step spacing (i.e. with the charge modulation) of the substrate. If, however, lattice matching with the original substrate surface is not fulfilled, adsorbate-induced faceting is an effective pathway to establish facet orientations which again allow for a lattice matching with enhanced interfacial stability. Such a situation has been observed previously for the system *NaCl on Cu(211)* [FHZ$^+$00, FHR$^+$02]. In this case, stripe-like (311)-oriented facets are formed which are selectively overgrown by the alkali halide. These facets are separated by bare metal facets which are (111)-oriented. In this chapter it will be verified if this faceting process is also applicable to other insulator/metal combinations which are (i) characterized by similar geometrical properties, and which (ii) provide sufficient substrate surface mobility to enable the reorganization. Such a combination is given by the system **KCl on Ag(211)**. The decisive geometric quantities are the distance $d_{AH\langle 110\rangle}$ between identical ions in the (100)-terminated alkali halide layer along the polar $\langle 110\rangle$ in-plane direction and the intrinsic step separation of the (311) metal facet, $d_{metal(311),intr.steps}$:

$$\frac{d_{Cu(311),intr.steps}}{d_{NaCl\langle 110\rangle}} = \frac{4.23\,\text{Å}}{3.99\,\text{Å}} = 1.06 \approx \frac{d_{Ag(311),intr.steps}}{d_{KCl\langle 110\rangle}} = \frac{4.78\,\text{Å}}{4.45\,\text{Å}} = 1.07. \tag{5.1}$$

As evident from this ratio, the NaCl film on the Cu(311) facet is under a uniaxial strain of 6% perpendicular to the intrinsic Cu steps. Despite this geometrical mismatch, there is an epitaxial growth of the alkali halide film on this facet. The same can be expected to occur also for a KCl overlayer on a Ag(311) facet.

The investigations of the KCl/Ag(211) system in this chapter were performed by SPA-LEED.

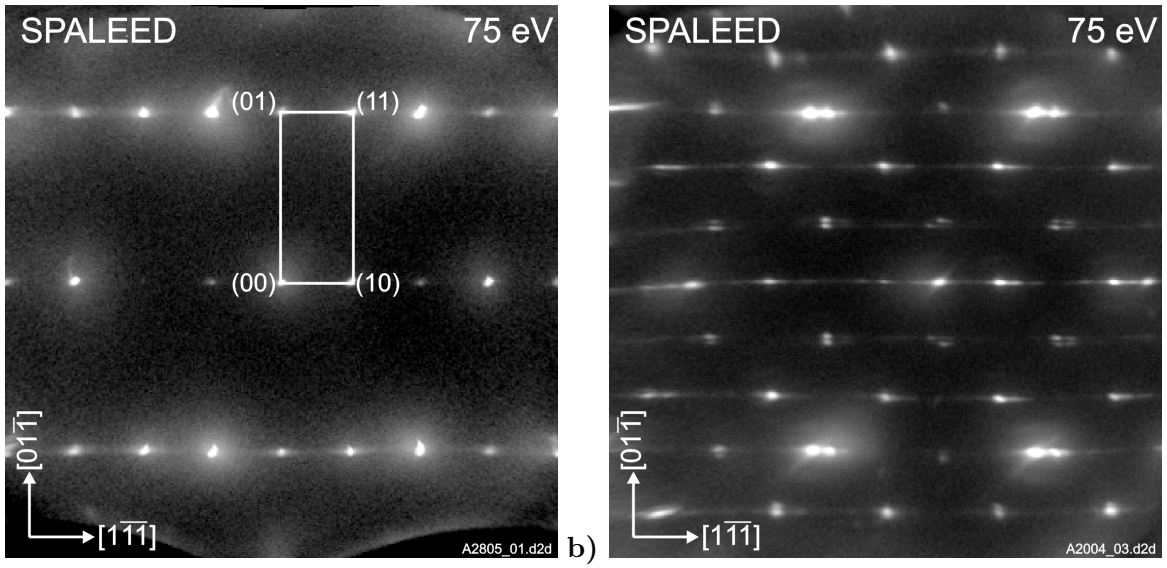

a) b)

Figure 5.1: a) LEED pattern of the clean Ag(211) surface taken at 75 eV with rectangular unit cell
b) LEED pattern taken at 75 eV of the completely faceted Ag(211) surface with 0.6 monolayers KCl deposited at 400 K; for all spots observed, the position with respect to $k_{\parallel}$ is dependent on the electron energy

5.1 KCl on Ag(211)

After preparing the Ag(211) sample according to the method described in section 1.3, a (1 × 1) LEED pattern with bright spots was observed (cf. Figure 5.1a). From the half width of the specular beam at an out-of-phase condition the average terrace width was estimated to ∼160 Å along the $[1\bar{1}\bar{1}]$ direction perpendicular to the intrinsic Ag steps, and ∼200 Å along the $[01\bar{1}]$ direction parallel to the intrinsic steps.

The investigation of the KCl growth mode on the Ag(211) surface was carried out by depositing 0.6 monolayers at substrate temperatures between 330 K and 470 K with a rate of 0.4 ML per minute. The result of the deposition of 0.6 ML KCl at 400 K substrate temperature can be seen in the LEED pattern in Figure 5.1b taken at 75 eV. The position of all observed spots with respect to $k_{\parallel}$ are, in contrast to the LEED pattern of the clean Ag(211) surface, dependent on the electron energy. Two sets of spots can be observed, the first set virtually moves in the $[1\bar{1}\bar{1}]$ direction (from left to right) with increasing energy, while the second set moves in the $[\bar{1}11]$ direction (from right to left). This indicates the formation of two different facet orientations.

A thorough determination of the LEED intensity as a function of $k_{\perp}$ and $k_{\parallel}$ pointing along the $[1\bar{1}\bar{1}]$ direction reveals the facet orientations formed during the present restructuring process. Figure 5.2 shows the result of such a measurement as a gray scale plot. It is observed that no

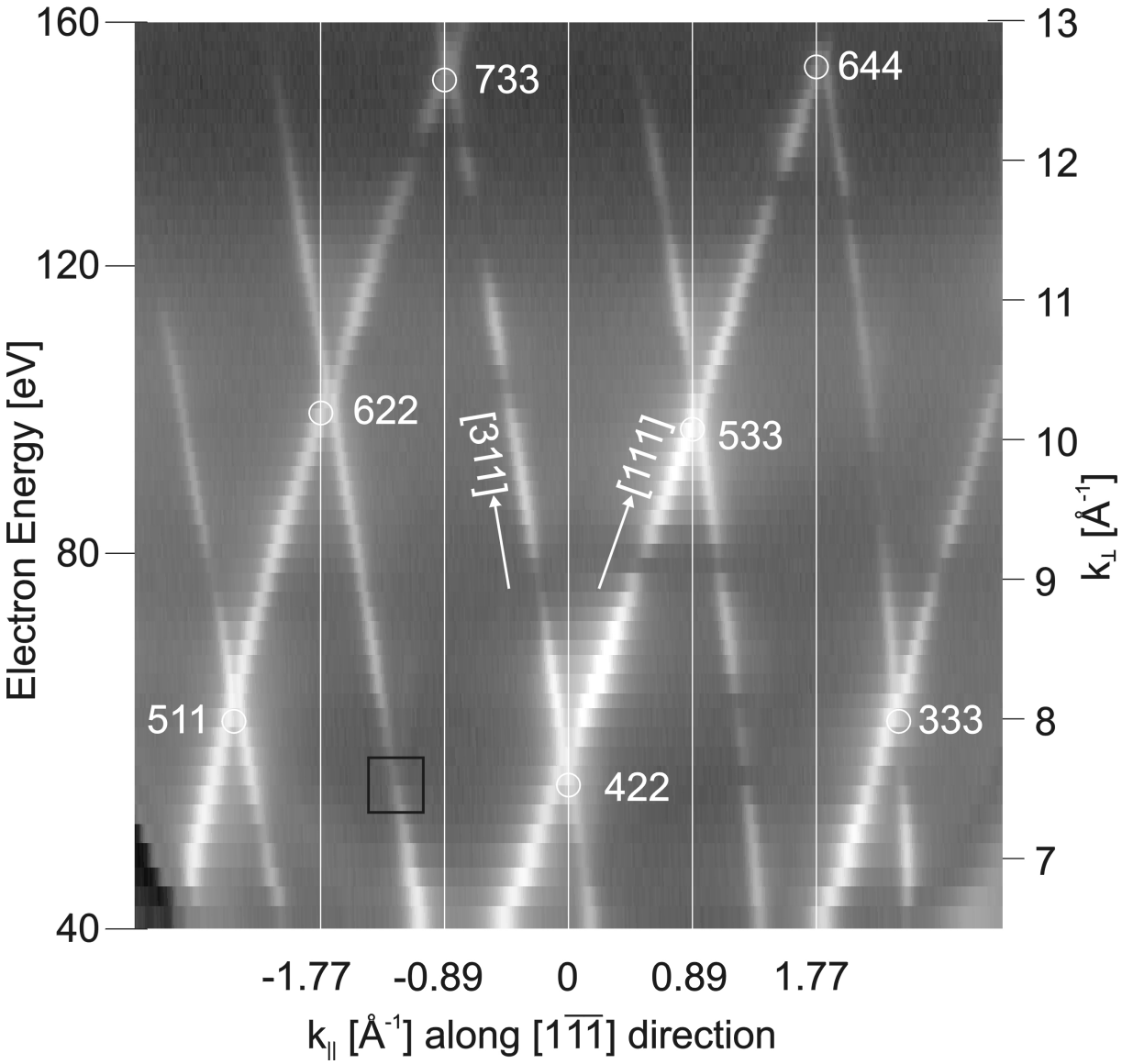

Figure 5.2: Gray scale plot of the LEED intensity I($k_\perp$,$k_\parallel$) of the faceted Ag(211) surface after the deposition of 0.6 monolayers KCl at 400 K substrate temperature
all intensity is confined to the tilted facet rods belonging to the (311) and the (111) orientation; no intensity is visible along the original (211) lattice rods (white vertical lines) indicating that the whole surface is faceted; the sharpness of the facet rods indicates flat facets with a high degree of long-range order; due to the distortion for larger $k_\parallel$, the lattice rods are omitted in this region

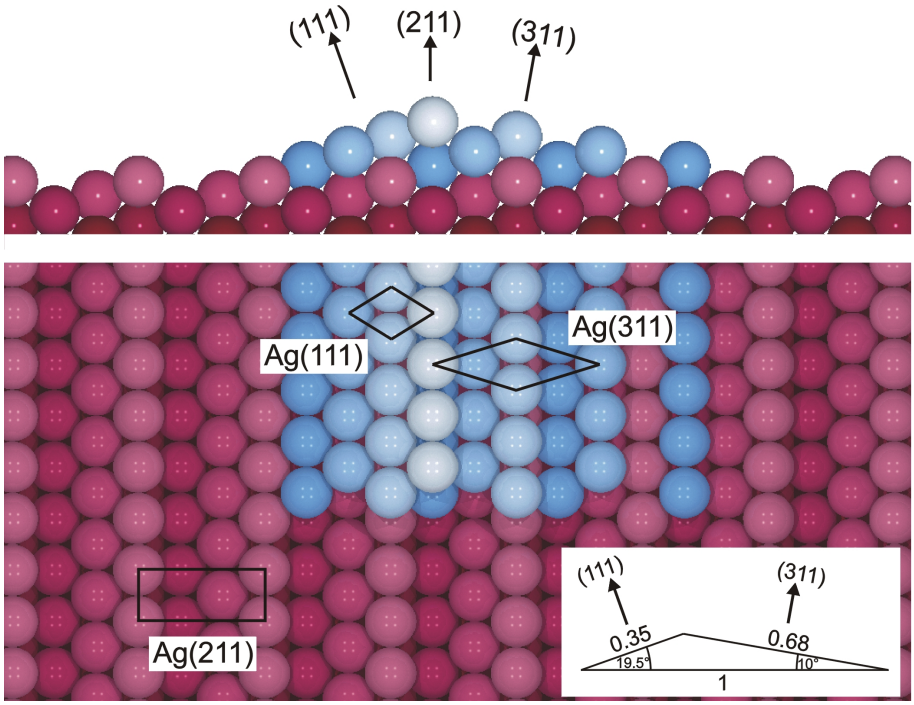

Figure 5.3: Hard-sphere model of the facet structure
bottom: original (211) surface with the rectangular unit cell
middle: facet structure with (111) and (311) facets (only the faceted template is drawn into the model; the KCl adlayer which causes the faceting process is omitted for clarity)
top: side view of the faceted structure with the (111) and the (311) facet
small inset in lower right corner: geometrical relation between the substrate and the facet orientations

intensity is found along the lattice rods corresponding to the original Ag(211) surface (white vertical lines in Figure 5.2), which indicates that the whole surface is faceted. The essential result of this plot is that there are two facet orientations indicated by their respective facet rods. From the indexing of the Bragg points where the facet rods intersect, the orientations of the facets are easily determined and correspond to the (311) and the (111) direction. The fact that sharp facet rods are observed for all scattering conditions indicates that the facets are atomically flat and have a high degree of long-range order [Hen84, Hor99].

The structure model derived from this analysis can be seen in Figure 5.3. For clarity, this hard-sphere model shows only the substrate atoms and the additional adlayer atoms are omitted. In the lower panel of the figure one can see the original (211) surface (cf. red spheres) together with additional atom rows (cf. blue spheres) to build up the observed faceted structure. The top part shows a side view of the facet structure (viewed along the step direction) with the (111) facet on the left and the (311) facet on the right. The inset in the lower right corner emphasizes

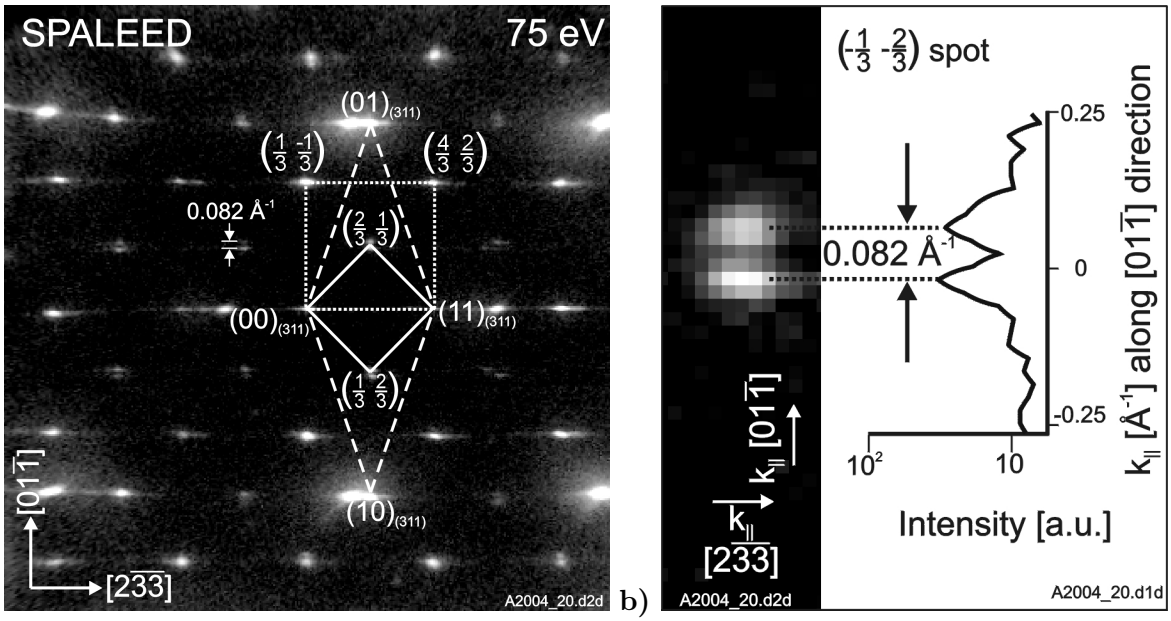

Figure 5.4: a) LEED pattern taken at 75 eV of the Ag(311) facet after deposition of 0.6 monolayers KCl at 400 K with $k_\perp$ parallel to the normal of the (311) facet
the Ag(311) unit cell (dashed line) and the bulk terminated p(1 × 1) KCl unit cell (dotted line) are drawn into the LEED pattern; the spots in c(2 × 2) superstructure (solid line) are induced by the KCl adlayer; the spot splitting measures 0.082 $Å^{-1}$ in the [01$\bar{1}$] direction, i.e. parallel to the intrinsic steps
b) the respective line scan of the $(-\frac{1}{3} \; -\frac{2}{3})$ spot shows the spot splitting along the step direction in detail

the geometry of the facet structure. The (111) facet is inclined by 19.5° with respect to the (211) surface and has a fractional surface area of 0.35, whereas the (311) facet is inclined by 10° and has a fractional surface area of 0.68.

The structure of the two facet orientations was investigated in detail by rotating the sample in such a way that the scattering vector component $k_\perp$ is parallel to the respective facet normal. For the two cases the respective LEED patterns are shown in Figure 5.4a (with $k_\perp$ parallel to the (311) facet normal) and Figure 5.6 (with $k_\perp$ parallel to the (111) facet normal). If one chooses this measurement geometry, the $k_\parallel$-dependent position of one set of diffraction spots does not change with the electron energy while the other set changes its position when varying the energy.

Figure 5.4a, where the $k_\perp$ component of the scattering vector is parallel to the (311) facet normal, is used to analyze this facet. The spots which are fixed in their position with respect to $k_\parallel$ reflect the interfacial geometry between the Ag(311) facet and the (100) terminated KCl adlayer on this facet. In analogy to the system NaCl/Cu(311), a c(2 × 2) superstructure (unit

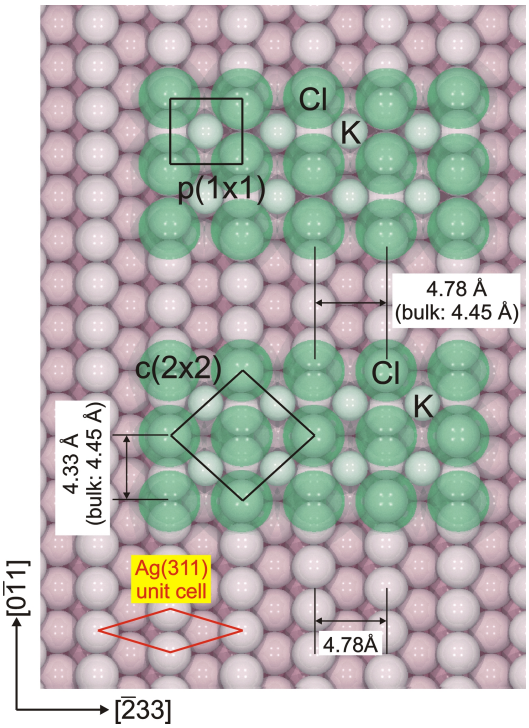

Figure 5.5: Hard-sphere model of the KCl-covered Ag(311) facet
bottom: (311) facet with the rhombic primitive unit cell
middle: KCl in c(2 × 2) configuration; the Cl ions are in alternating on-top and bridge positions along the intrinsic steps
top: KCl in p(1 × 1) configuration; the Cl ions are shifted along the intrinsic steps by $\frac{1}{4}$ of the Ag-Ag spacing with respect to the c(2 × 2) configuration; all Cl ions are at equivalent positions with respect to the underlying (311) template

cell indicated by the full line) is observed (cf. section 4.1). The Ag(311) unit cell (dashed line) and the bulk terminated p(1 × 1) KCl unit cell (dotted line) are also indicated in the LEED pattern. Additionally, a spot splitting of 0.082 Å^{-1} in the direction parallel to the intrinsic Ag steps is found.

Obviously, the adlayer configuration of KCl on the Ag(311) facet has the following features in common with the system NaCl on Cu(311): The polar ⟨110⟩ in-plane directions of the alkali halide adlayer are parallel and perpendicular to the intrinsic Ag steps and – due to the Smoluchowski effect – the Cl ions are located on top of these steps while the K ions are located in the troughs. Consequently, the Cl-Cl spacing perpendicular to intrinsic steps corresponds to 4.78 Å (KCl bulk value: 4.45 Å). The hard-sphere model for the adlayer configuration of KCl/Ag(311) is shown in Figure 5.5. At the bottom, the Ag(311) unit cell (small rhombus) is indicated. The c(2 × 2) configuration can be seen in the middle of the model. This configura-

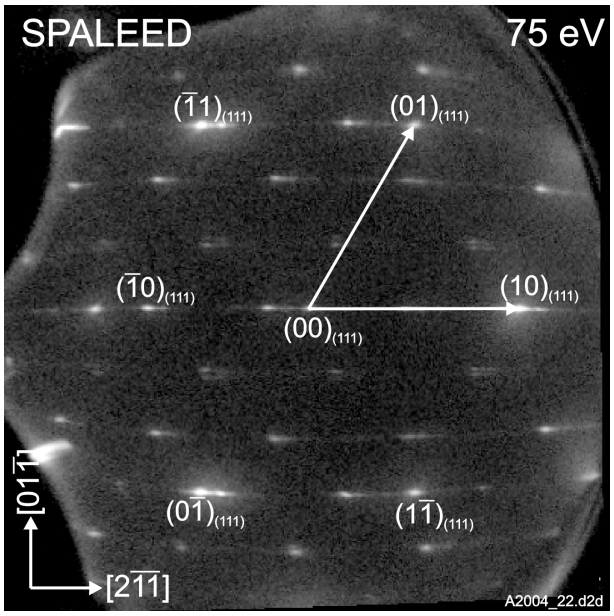

Figure 5.6: LEED pattern taken at 75 eV of the faceted Ag(211) surface after deposition of 0.6 monolayers KCl at 400 K with $k_\perp$ normal to (111) facet
labeled are the seven, visible spots belonging to the Ag(111) facet and two surface base vectors in reciprocal space; no additional spots occur, which are fixed in their position with respect to $k_\parallel$ while changing the electron energy

tion is characterized by Cl ions in alternating on-top and bridge positions with respect to the underlying close-packed Ag rows. At the top, the p(1 × 1) configuration is illustrated, where the Cl ions are shifted along the intrinsic rows by $\frac{1}{4}$ of an Ag-Ag spacing with respect to the c(2 × 2) configuration. For both configurations, the Cl-Cl distance $a_{KCl,\parallel}$ parallel to the intrinsic steps would be 4.33 Å = 1.5 × 2.88 Å (Ag-Ag spacing $a_{Ag,\parallel}$) for a locally commensurate matching. The antiphase domain disorder which leads to the observed spot splitting of 0.082 $Å^{-1}$ (cf. Figure 5.4b) allows for the adjustment of a relaxed Cl-Cl spacing along the intrinsic Ag steps, as discussed in detail in conjunction with the growth systems presented in chapter 4. The spot splitting corresponds to a periodic length of L=77 Å for the mean separation of two adjacent domains with the same superstructure. For a sequence of alternating p(1 × 1) and c(2 × 2) domains the Cl ions are shifted by one half Ag-Ag spacing relative to the substrate between two adjacent domains of identical superstructure. Therefore, the Cl-Cl spacing can be calculated as $a_{KCl,\parallel} = 1.5 a_{Ag,\parallel} \left[1 \pm \left(\frac{a_{Ag,\parallel}/2}{L}\right)\right]$. An expansion of the KCl layer with respect to a locally commensurate configuration leads to a Cl-Cl distance of 4.41 Å, whereas for a contraction the Cl-Cl spacing would be 4.25 Å.

The LEED pattern in Figure 5.6, for which the $k_\perp$ component of the scattering vector is

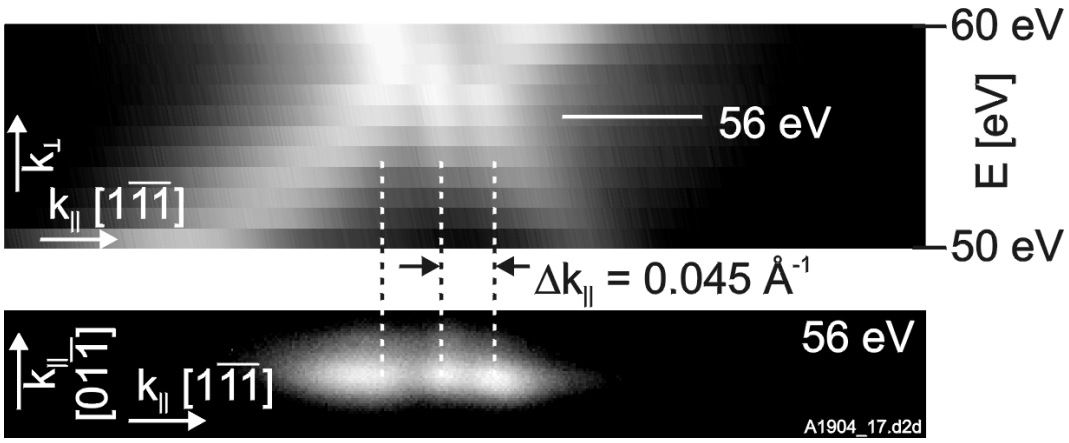

Figure 5.7: Diffraction data of the faceted Ag(211) surface with 0.6 ML KCl deposited at 370 K
top: gray scale plot of the LEED intensity $I(k_\perp,k_\parallel)$ for electron energies between 50 eV and 60 eV; visible is the splitting of the rods of 0.045 $Å^{-1}$ in $[1\bar{1}\bar{1}]$ direction close to the in-phase energy of 56 eV
bottom: LEED pattern at 56 eV with the respective spot splitting

perpendicular to the (111) facet, is used to analyze the second facet. The spots belonging to this facet are hexagonally arranged with the reciprocal translation indicative for Ag(111) (2.51 $Å^{-1}$). Only these seven spots (cf. labeling in the diffraction pattern) are fixed in their position with respect to $k_\parallel$ with changing electron energy. This indicates that the (111) facet is not covered with a KCl adlayer, and the facet is still bare Ag, which is equivalent to the findings in the system NaCl/Cu(211) [FHR+02].

An important morphological feature to investigate for this structure is the size-dependence of the facets on the substrate temperature (i.e. the substrate atom mobility during the faceting process). For scattering conditions close to the in-phase energy, LEED is sensitive to the large scale lateral roughness of a quasi-periodic facet array [WLH98], which leads to a spot splitting in the diffraction pattern (cf. Figure 5.7). The mean separation of the facets $\langle\Lambda\rangle$ is given by the spot splitting $\Delta k_\parallel$ close to the in-phase energy: $\langle\Lambda\rangle = \frac{2\pi}{\Delta k_\parallel}$. The in-phase energy for the Bragg point Ag(422) is 54 eV. Close to this energy the values for the spot splitting $\Delta k_\parallel$ were determined for different deposition temperatures. An exemplary beam profile for a deposition temperature of 370 K is shown in Figure 5.7. The width Γ of the (311) facet is determined from the half width of the specular lattice rod at 56 eV. This corresponds to the out-of-phase scattering condition midway between the (311) and the (622) Bragg point as indicated by the black square in Figure 5.2. For complete faceting into (311) and (111) facets – at coverages of about 0.6 monolayers – the ratio between the width Γ of the (311) facet and the mean separation Λ is given by 0.68 (cf. inset in the lower right corner of Figure 5.3).

Temperature [K]	$\Delta k_{\parallel}$ at 56 eV [Å^{-1}]	$\langle\Lambda\rangle$ [Å]	κ at 56 eV [Å^{-1}]	$\langle\Gamma\rangle$ [Å]	$\Delta k_{\parallel}/\kappa$
330	0.048	131	0.085	73	0.56
350	0.043	147	0.057	110	0.75
370	0.045	139	0.073	86	0.62
400	0.044	141	0.071	88	0.63
430	0.043	144	0.069	91	0.63
470	0.040	158	0.057	110	0.70

Table 5.1: Investigation of the facet size dependence on the temperature at a coverage of 0.6 ML KCl
$\Delta k_{\parallel}$ denotes the spot splitting in $[1\overline{1}1]$ direction close to the in-phase energy of 56 eV
$\langle\Lambda\rangle = \frac{2\pi}{\Delta k_{\parallel}}$ is the mean separation of the facets
κ is the half width of the (311) facet rod at 56 eV (cf. black square in Figure 5.2)
$\langle\Gamma\rangle = \frac{2\pi}{\kappa}$ is the average (311) facet width
$\Delta k_{\parallel}/\kappa$ is the ratio between the facet separation and the (311) facet width, which would be 0.68 in the case of complete faceting (cf. small inset in Figure 5.3)

In Table 5.1 the values for the mean separation, the width of the (311) facet, and their ratio for coverages of 0.6 ML at different temperatures are summarized. For the system KCl/Ag(211) only a weak dependence of the facet size on the temperature could be found. The experimental values obtained for 350 K do not fit in the monotonous increase in facet size with increasing deposition temperature. It is assumed that a measurement error occurred for this particular data set at 350 K so that these values are not considered. The observed increase of facet size with temperature is only moderate in comparison with that found for the system NaCl/Cu(211), where an increase of the facet size by a factor of three occurs over the same temperature range [FHR^{+}02].

This behavior indicates that the faceting process is not only kinetically limited by the mobility of the substrate adatoms. At the starting temperature of 330 K the mobility is high enough to form (311) facets with the width of about 100 Å. Also for higher mobility (due to higher substrate temperature) the facets formed are not significantly larger. Obviously, there are additional contributing factors that determine the facet size. As a potential mechanism, the facet formation could be limited by the uniaxial strain of the KCl adlayer (Cl-Cl distance in bulk: 4.45 Å) perpendicular to the steps of the Ag(311) facet (distance between intrinsic steps: 4.78 Å). The mismatch of about 7 % which is larger by 1% compared to the mismatch observed for the system NaCl/Cu(211) can be of significance for the observed restraint in facet size.

The overall faceting mechanism for the system KCl/Ag(211) can be described as follows: By deposition up to 0.6 monolayers of KCl onto the Ag(211) surface a self-organized restructuring

process takes place. The initially flat surface reorganizes into KCl-covered (311) facets and bare Ag(111) facets. The energetic driving force is the enhanced interfacial stability between the Ag(311) facet and the (100)-oriented KCl adlayer. The configuration of the monomolecular KCl adlayer on the Ag(311) facet is similar to the NaCl adlayer on the Cu(311) template. Due to the Smoluchowski effect Cl ion rows of the film match with the location of the intrinsic steps of the Ag(311) facet. Parallel to the intrinsic steps, on the other hand, the adlayer adopts a relaxed Cl-Cl spacing. It is shown that the present faceting mechanism is applicable to systems with different substrate and deposit materials which fulfill a similar geometrical relationship. These systems are e.g. NaCl/Cu(211), which was studied previously in our group [RFMR01, FHR$^+$02], and KCl/Ag(211), which was shown here.